Characterization of Peptidoglycan in *Fem*-Deletion Mutants of Methicillin-Resistant *Staphylococcus aureus* by Solid-State NMR[†]

Shasad Sharif,[‡] Sung Joon Kim,[‡] Harald Labischinski,[§] and Jacob Schaefer*[,‡]

Department of Chemistry, Washington University, One Brookings Drive, St. Louis, Missouri 63130, and MerLion Pharmaceuticals GmbH, Robert-Rössle-Strasse 10, 13125 Berlin, Germany

Received September 13, 2008; Revised Manuscript Received December 16, 2008

ABSTRACT: Compositional analysis of the peptidoglycan (PG) of a wild-type methicillin-resistant *Staphylococcus aureus* and its *fem*-deletion mutants has been performed on whole cells and cell walls using stable-isotope labeling and rotational-echo double-resonance NMR. The labels included [1-^{13}C,^{15}N]glycine and L-[ε-^{15}N]lysine (for a direct measure of the number of glycyl residues in the bridging segment), [1-^{13}C]glycine and L-[ε-^{15}N]lysine (concentration of bridge links), and D-[1-^{13}C]alanine and [^{15}N]glycine (concentrations of cross-links and wall teichoic acids). The bridging segment length changed from 5.0 glycyl residues (wild-type strain) to 2.5 ± 0.1 (FemB) with modest changes in cross-link and bridge-link concentrations. This accurate *in situ* measurement for the FemB mutant indicates a heterogeneous PG structure with 25% monoglycyl and 75% triglycyl bridges. When the bridging segment was reduced to a single glycyl residue 1.0 ± 0.1 (FemA), the level of cross-linking decreased by more than 20%, resulting in a high concentration of open N-terminal glycyl segments.

Methicillin-resistant *Staphylococcus aureus* (MRSA)[1] is the leading pathogen for nosocomial infections (*1*). The mechanism of β-lactam antibiotic resistance in MRSA is related to the chromosomal *mec* determinant containing gene *mecA* (*2*), which encodes the low-affinity penicillin-binding protein PBP2a (alternatively termed PBP2′) that participates in cell-wall biosynthesis (*3*). The level of β-lactam antibiotic resistance in MRSA also depends on *fem* (factors essential for methicillin resistance) factors (*4*−*6*), also called *auxiliary* factors (*7*), that are unrelated to the *mec* determinant (*2*). *Fem* factors are known to affect β-lactam antibiotic resistance in MRSA indirectly through cell-wall metabolism (*4*−*6*). Some of these *fem* factors include *femX*, *femA*, and *femB*, which encode proteins FemX, FemA, and FemB, respectively. These Fem proteins are involved in peptidoglycan (PG) biosynthesis by enabling the sequential addition of glycines to the lysyl side chain of the PG stem of lipid II, the membrane-associated PG precursor which is attached to the lipid transporter C_{55} (pyrophosphoryl-undecaprenol). FemX (*8, 9*) presumably catalyzes the addition of the first glycyl unit, FemA (*10*−*12*) the second and third units, and FemB (*13*) the fourth and fifth glycyl units to complete the pentaglycyl bridge structure of the PG unit in lipid II. Complete *femAB* inactivation results in a FemAB null mutant (*14*−*16*), which has a structure similar to that of FemA.

Lipid II is the essential precursor required for transglycosylation, the incorporation of a PG unit to the growing linear glycan chain. The chemical structure of a repeating PG unit in *S. aureus* (Scheme 1, right panel) consists of a disaccharide, *N*-acetylglucosamine (GlcNAc) plus *N*-acetylmuramic acid (MurNAc), and a pentapeptide stem (L-Ala-D-*iso*-Gln-L-Lys-D-Ala-D-Ala), with an attached pentaglycyl bridging segment (*17*). Transpeptidase transforms linear glycan chains to a three-dimensional meshed PG lattice by forming cross-links (*2*). Each cross-link is a peptide bond formed between the terminal glycine of the bridging segment of one glycan chain and the D-alanine (the fourth amino acid) of the stem of an adjacent glycan chain. The terminal D-alanine (the fifth amino acid) of the stem is cleaved by transpeptidase upon formation of a cross-link. A schematic representation of a meshed PG structure for *S. aureus* and its *fem*-deletion mutants is shown in Scheme 1 (left panel).

The deletion of *femX* in *S. aureus* is lethal (*8, 9*), whereas the deletion of *femA* and *femB* results in biosynthesis of precursors with PG bridge segments consisting of mono- and triglycyl segments, respectively (*4*−*6*). Shortened bridging segments result in reduced separation between the adjacent glycan chains (Scheme 1). Hence, the PG tertiary structures of *fem*-deletion mutants are likely to differ from that of wild-type *S. aureus*. These variations are consistent with reduced sensitivity to lysostaphin digestion (*4, 5*), a glycine-glycine endopeptidase which selectively cleaves the PG bridges. Therefore, the use of *S. aureus* and its isogenic *fem*-deletion mutants provides a unique opportunity to investigate the role

[†] This paper is based on work supported by National Institutes of Health via Grant EB002058.

* To whom correspondence should be addressed. Phone: (314) 935-6844. Fax: (314) 935-4481. E-mail: jschaefer@wustl.edu.

[‡] Washington University.

[§] MerLion Pharmaceuticals GmbH.

[1] Abbreviations: C_{55}, pyrophosphoryl-undecaprenol; CPMAS, cross-polarization magic-angle spinning; *fem*, factors essential for methicillin resistance; GEU, glycine-equivalent unit; lipid II, *N*-acetylglucosamine-*N*-acetyl-muramyl-pentapeptide-pyrophosphoryl-undecaprenol; MAS, magic-angle spinning; MIC, minimum inhibitory concentration; MRSA, methicillin-resistant *S. aureus*; PBP, penicillin-binding protein; PG, peptidoglycan; REDOR, rotational-echo double resonance; SASM, *S. aureus* standard medium; SSB, spinning-sideband; TEM, transmission electron micrograph; TSB, trypticase soy broth.

10.1021/bi801750u CCC: $40.75
Published on Web 03/23/2009

Scheme 1: (Left) Schematic Representation of an Idealized Cell-Wall Peptdioglycan of *S. aureus* and Its *fem*-Deletion Mutants[a] and (Right) Chemical Structure of the Peptidoglycan Stems in the Peptidoglycan of *S. aureus* and Its *fem*-Deletion Mutants

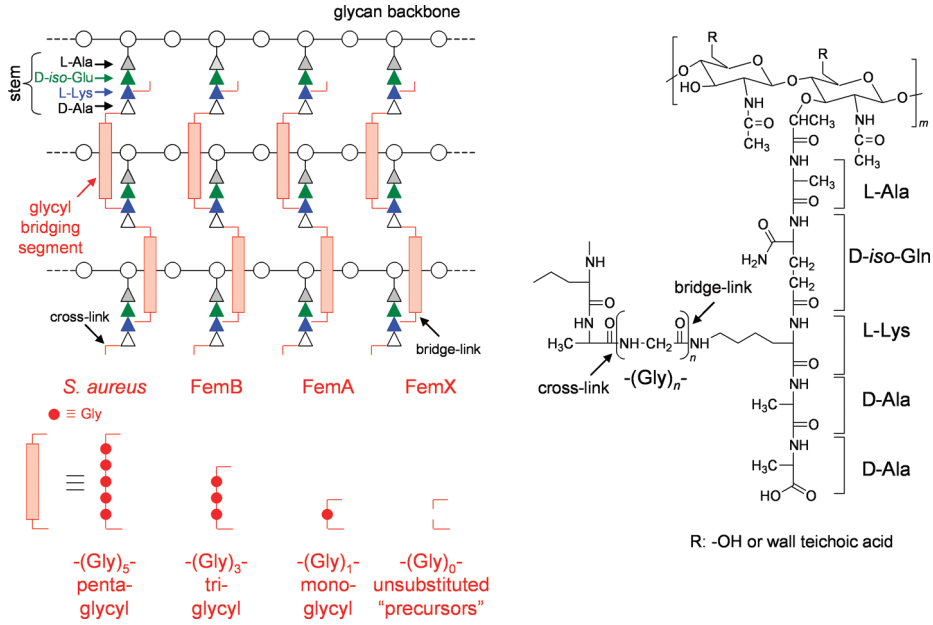

[a] A four-unit peptide stem (triangles) having the sequence L-Ala-D-*iso*-Gln-L-Lys-D-Ala is attached to every second sugar of the glycan backbone (○). Cross-linking between glycans occurs through glycyl side chains (red circles) connecting the carbonyl carbon of D-Ala of the fourth position of one stem to the ε-nitrogen (in an isopeptide bond) of L-Lys of the third position of another. The glycine content in the side chain varies from pentaglycyl (*S. aureus*), triglycyl (FemB), and monoglycyl (FemA) to an accumulation of unsubstituted precursors with no bridges (FemX).

of bridge length on the PG tertiary structure. The bridges are systematically varied from penta- to tri- to monoglycyl segments, while other enzymatic steps in PG biosynthesis are constant.

Our long-range goal is to understand the effect of bridge length on the three-dimensional PG lattice in *S. aureus*. This will be accomplished using solid-state NMR in two steps: (i) determination of the PG composition of whole cells of a wild-type *S. aureus* (*18*) and its *femX* (*8, 9*), *femA*-deletion (*10*−*12*), and *femB*-deletion (*13*) mutants (Table S1 of the Supporting Information) and (ii) investigation of the PG tertiary structure of these bacteria. In this report, we describe the use of solid-state NMR to characterize the composition of intact cell walls in wild-type *S. aureus* and its *fem*-deletion mutants by determining the number of glycines in the PG bridge, the degree of bridge-linking (ρ_{BL}), the degree of cross-linking (ρ_{CL}), and the average cross-link density (ρ). The analysis of PG composition of intact cell walls of these bacteria is the necessary first step for the subsequent investigation of PG tertiary structure in which ^{19}F-labeled glycopeptides are used as molecular NMR probes to examine structural trends in the same intact cell walls, to provide new insights into the assembly of the PG lattice, and to understand the mode of action of drugs that bind to the cell-wall lattice (*19, 20*).

EXPERIMENTAL PROCEDURES

Growth and Labeling of Whole Cells of Wild-Type, FemA, and FemB S. aureus. Starter cultures of wild-type *S. aureus* (BB255) (*18*) and its *FemA* (UK 17) (*10*−*12*) and *FemB* (UT 34-2) (*13*) mutants, listed in Table S1 of the Supporting Information, were prepared by inoculating 5 mL of trypticase soy broth (TSB) in a test tube with a single colony obtained from a nutrient agar plate. The starter cultures were shaken at 200 rpm in an Environ-Shaker (Laboratory-Lines Instruments, Inc., Melrose Park, IL), maintained overnight at 37 °C, but not aerated. The overnight starter culture (1% final volume) was added to 2 L of sterile *S. aureus* standard medium (SASM), in six 1 L flasks each containing 330 mL. SASM, as described previously by Tong et al. (*21*), contained the following on a per-liter basis: 10 g of D-(+)-glucose; 1 g each of $K_2HPO_4 \cdot 3H_2O$, KH_2PO_4, and $(NH_4)_2SO_4$; 0.2 g of $MgSO_4 \cdot 7H_2O$; 10 mg each of $MnSO_4 \cdot H_2O$, $FeSO_4 \cdot H_2O$, and NaCl; 5 mg each of adenine, cytosine, guanine, uracil, and xanthine; 2 mg each of thiamine·HCl (vitamin B_1), niacin (vitamin B_3), and calcium pantothenate (vitamin B_5); 1 mg each of riboflavin (vitamin B_2), pyridoxine·HCl (vitamin B_6), inositol, $CuSO_4 \cdot 5H_2O$, and $ZnSO_4 \cdot 7H_2O$; 0.1 mg each of biotin (vitamin B_7) and folic acid (vitamin B_9); and 0.1 g of all 20 common amino acids. The pH of SASM was adjusted to 7.0 with 1 M KOH, followed by sterile filtration (0.22 μm membrane).

The natural-abundance amino acids in SASM were replaced with either [1-^{13}C,^{15}N]glycine and L-[ε-^{15}N]lysine, [1-^{13}C]glycine and L-[ε-^{15}N]lysine, or [^{15}N]glycine and D-[1-^{13}C]alanine, to incorporate specific ^{13}C and ^{15}N labels (Cambridge Isotope Laboratories, Inc., and Isotec) in the glycyl bridging segments, bridge-links, or cross-links, respectively, in the PG of whole cells (Scheme 1).

The cells were harvested at log phase at an optical density (OD) of 0.6 at 660 nm by centrifugation at 10000*g* for 10 min at 4 °C in a Sorvall GS-3 rotor. Cell pellets were rinsed twice with 300 mL of ice-cold 40 mM triethanolamine hydrochloride (pH 7.0, adjusted with 1 M NaOH). The rinsed pellets were resuspended in 15 mL of the same buffer followed by rapid freezing and lyophilization. The resulting lyophilized whole cells

harvested from 2 L of growth typically weighed 400 mg. Growth curves of wild-type *S. aureus* (BB255) and its FemA (UK 17) and FemB (UT 34-2) mutants in SASM are shown in Figure S1 of the Supporting Information.

Growth and Labeling of Whole Cells of FemX S. aureus. Because the inactivation of *fmhB* (postulated *femX* gene) is lethal (*9*), the *fmhB*-deletion mutant (SR 18) contains a temperature-sensitive plasmid with the *fmhB* gene under the regulation of a xylose promoter with erythromycin resistance (*8*). To ensure the integration of the temperature-sensitive plasmid, all SR 18 growths were carried out at 42 °C in the presence of 10 μg/mL erythromycin (Sigma-Aldrich) in both solid and liquid media. The whole-cell samples were prepared by inoculating 1 L of SASM (three 1 L flasks, each containing 330 mL) with an overnight starter culture of SR 18 grown in LB broth supplemented with either 0.5% D-(+)-glucose or D-(+)-xylose. SASM contained either 1% D-(+)-glucose or D-(+)-xylose as the sole carbon source to enhance or to repress the *fmhB* expression, respectively. The natural-abundance glycine and lysine in SASM were replaced with labeled [1-^{13}C]glycine and L-[ε-^{15}N]lysine, respectively. Whole cells were harvested at an $OD_{660\,nm}$ of 0.6 and subsequently prepared and lyophilized as described previously (*20, 21*). The resulting lyophilized whole cells harvested from 1 L of growth typically weighed 200 mg. The growth curve of SR 18 in SASM is shown in Figure S1 of Supporting Information.

Isolation of Peptidoglycan. Cell-wall isolates were prepared from lyophilized whole cells as previously described (*20, 21*). Briefly, lyophilized cells from the 2 L of log-phase growth were suspended in 100 mL of sterile 0.025 M potassium phosphate buffer (pH 7.0), boiled for 30 min, and then chilled on an ice bath. To the cell suspension was added DNase I (type II; from bovine pancreas, Sigma-Aldrich, 1 mg per 100 mg of dry cell weight), and the mixture was transferred to a 250 mL Bead-Beater (Biospec Products, Bartlesville, OK) chamber containing one-third 0.5 mm diameter glass beads. Cell disruption employed ten 1 min cycles separated by 1 min cooling periods at 0 °C. Glass beads were separated from the broken cells with a coarse sintered glass funnel (20 μm). The cells were washed with 1 L of 10 mM EDTA. Centrifugation of the filtrate at 10000*g* for 1 h at 4 °C provided crude cell walls.

Cell-wall isolates for NMR analysis were obtained from a suspension of the crude cell-wall pellet in a minimum amount of sterile 10 mM triethanolamine hydrochloride buffer (pH 7.0, adjusted with 1 M NaOH), which was added dropwise with stirring to 100 mL of boiling 4% sodium dodecyl sulfate (SDS). After being boiled for 30 min, the suspension was allowed to cool for 2 h with stirring, after which it was allowed to stand unstirred overnight at room temperature, and sedimented by centrifugation at 38000*g* for 1 h at room temperature in a Sorvall SS-34 rotor. Walls were rinsed with 100 mL of buffer at least four times, with centrifugation after each rinse, until no SDS could be observed. The pellet was resuspended in 60 mL of 0.01 M Tris buffer (pH 8.2) containing 1 mg per 100 mg of dry cell weight DNase I and 3.2 mg per 100 mg of dry cell weight of trypsin (type II-S; from bovine pancreas, Sigma-Aldrich) and α-chymotrypsin (type II; from bovine pancreas, Sigma-Aldrich). The suspension was incubated at 37 °C, shaken at 150 rpm in an Environ-Shaker for 16 h, then sedimented at 38000*g* for 1 h at 20 °C, and washed at least four times with buffer, with centrifugation after each rinse. Cells were then resuspended in a minimum amount of 12 mL of the same buffer followed by rapid freezing and lyophilization. The resulting cell-wall isolates weighed approximately 150 mg.

Transmission Electron Microscopy. Overnight starter cultures of wild-type BB255 and FemA and FemB mutants of *S. aureus* grown in TSB were used to inoculate 40 mL of sterile SASM (1% final volume) in 125 mL flasks. Cells were grown at 37 °C, shaken at 200 rpm in an Environ-Shaker, and harvested at log phase until an $OD_{660\,nm}$ of 0.2 was reached by centrifugation at 2750*g* for 20 min at 4 °C (Eppendorf Centrifuge 5810R). For ultrastructural analysis, bacteria were fixed in 1 mL of a 2% paraformaldehyde/2.5% glutaraldehyde mixture (Polysciences Inc.) in 100 mM phosphate buffer (pH 7.2) for 3 h at room temperature. Samples were washed in phosphate buffer and postfixed in 1% osmium tetroxide (Polysciences Inc.) for 1 h. Samples were then rinsed extensively in distilled water prior to enbloc staining with 1% aqueous uranyl acetate (Ted Pella Inc.) for 1 h. Following several rinses in distilled water, samples were dehydrated in a graded series of ethanol and embedded in Eponate 12 resin (Ted Pella Inc.). Sections of 95 nm were cut with a Leica Ultracut UCT ultramicrotome (Leica Microsystems Inc.), stained with uranyl acetate and lead citrate, and viewed on a JEOL 1200 EX transmission electron microscope (JEOL USA Inc.).

Solid-State NMR Measurements. Experiments were performed at 7 T (300 MHz for protons) and 12 T (500 MHz for protons) provided by 89 mm bore Oxford (Cambridge, U.K.) and Magnex (Oxfordshire, U.K.) superconducting solenoids, respectively. Experiments performed at 7 T used a four-frequency transmission-line probe (*22*) having a 14 mm long, 9 mm inner-diameter sample coil, and a Chemagnetics/Varian magic-angle spinning ceramic stator. Samples were spun in Chemagnetics/Varian 7.5 mm outer-diameter zirconia rotors at 5 kHz, with the speed under active control and maintained within ±2 Hz. Experiments were conducted at room temperature using a Chemagnetics CMX-300 spectrometer operating at 30 MHz for ^{15}N and 75 MHz for ^{13}C. Radiofrequency pulses were produced by 1 kW Kalmus, ENI, and American Microwave Technology power amplifiers, each under active control (*23*); π pulse lengths were 10 μs for ^{13}C and ^{15}N. Proton-carbon and proton-nitrogen matched cross-polarization transfers were at 50 kHz for 2 ms. The proton dipolar decoupling was 105 kHz during data acquisition.

Experiments performed at 12 T used a six-frequency transmission-line probe having a 12 mm long, 6 mm inner-diameter sample coil and a Chemagnetics/Varian ceramic spinning module. Samples were spun using a thin-wall Chemagnetics/Varian (Fort Collins, CO, or Palo Alto, CA) 5 mm outer-diameter zirconia rotor at 7143 Hz, with the speed under active control and maintained within ±2 Hz. A Tecmag Libra (Houston, TX) pulse programmer controlled the spectrometer. American Microwave Technology power amplifiers (2 kW) were used to produce radiofrequency pulses for ^{15}N (50 MHz) and ^{13}C (125 MHz). The ^{1}H (500 MHz) radiofrequency pulses were generated by 2 kW Creative Electronics tube amplifiers driven by a 50 W American Microwave Technology power amplifier. All

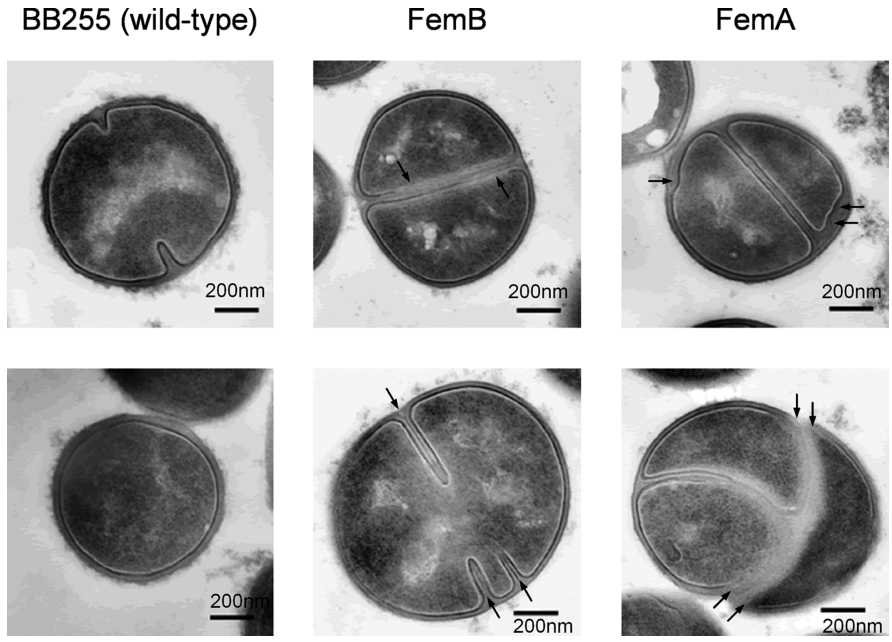

FIGURE 1: Transmission electron micrographs of whole cells of *S. aureus* grown in defined medium (SASM) and harvested at an OD of 0.2 at 660 nm: (left) wild-type BB255, (middle) FemB (UT 34-2), and (right) FemA (UK 17). The arrows indicate morphological irregularities for the mutant strains. The average cell size for the mutants are comparable to that of the wild-type strain.

amplifiers were under active control (*23*). The π pulse lengths were 8 μs for ^{13}C and 9 μs for ^{15}N. Proton-carbon matched cross-polarization transfers were conducted in 2 ms at 62.5 kHz. The proton dipolar decoupling was 100 kHz during data acquisition, and TPPM of the ^{1}H radiofrequency (*24*) was used throughout both dipolar evolution and decoupling periods.

Rotational-echo double resonance (REDOR) is a solid-state NMR technique used to recouple heteronuclear dipolar interactions under magic-angle spinning (MAS) (*25, 26*). REDOR experiments are performed in two parts: once with dephasing pulses (S) and once without (S_0). In the first part of the experiment, the dephasing pulses are off and magic angle spinning spatially averages chemical-shift and dipolar anisotropic interactions to produce a signal of full intensity. In the second part of the experiment, π pulses are applied on the dephasing channel to reintroduce the dipolar coupling between spins and produce a reduction in echo-signal intensity. The difference in signal intensity ($\Delta S = S_0 - S$) is directly related to the internuclear distance between the observed and dephasing spins. For the 1.2 kHz one-bond ^{13}C$-^{15}$N dipolar coupling in a labeled peptide bond, total dephasing is observed after $8T_r$ (1.60 ms) with 5 kHz MAS, or after $12T_r$ (1.68 ms) with 7143 Hz MAS. The effect of a second weaker coupling is negligible because of dipolar truncation (*27*). The uncertainty associated with the REDOR dephasing measurements was estimated by integrals of ΔS (*28*). For all ΔS spectra, the uncertainty was less than 1%. REDOR spectra typically consisted of 4098 acquisition scans for ^{13}C and 20000 acquisition scans for ^{15}N.

RESULTS

Transmission Electron Micrographs. Transmission electron micrographs (TEM) of ultrathin sections of wild-type *S. aureus* (BB255) and *FemA* (UK 17) and *FemB* (UT 34-2) mutants are shown in Figure 1. The cell-wall thickness of the wild type and the FemB mutant was in the range of 20 nm (Figure 1, left and middle). Only the FemA mutant exhibited partial cell-wall thickening with a maximum thickness measured at 67 nm, indicated by the arrows in Figure 1 (top right panel). The FemA mutant also exhibited diffused staining at cross walls thickened in a range of 50−70 nm. This suggested an accumulation of immature peptidoglycan at the septum in association with aberrant growth. Deformed cell morphologies and aberrant growths with multiple septum formation were observed in both *fem*-deletion mutants (arrows).

Glycine Content in Whole Cells. The 75 MHz ^{13}C{^{15}N} REDOR spectra of whole cells of wild-type *S. aureus* and its *fem*-deletion mutants, grown on SASM medium labeled with [1-^{13}C,^{15}N]glycine and L-[ε-^{15}N]lysine, after dipolar evolution for 1.60 ms, are shown in Figure 2. Signals from the sugars in the PG glycan backbone appear around 70 ppm (*29*), and from the aliphatic carbons, including the lipids from the membrane, between 20 and 40 ppm (*30*). The peak at 149 ppm is from [1-^{13}C]glycine metabolism in purine biosynthesis (*31*). The similarities of the wild-type and mutant natural-abundance ^{13}C spectral profiles, as well as the similar intensities of purine peaks, suggest that no significant cytoplasmic compositional variations are present in the *fem*-deletion mutants. However, the large decrease in the 171 ppm intensities in the S_0 spectra of FemB and FemA compared to that in wild-type *S. aureus* shows qualitatively a reduction in the number of glycines in the bridge structures.

Quantitative measurements of glycine content in PG bridging segments of wild-type and *fem*-deletion mutants were made using REDOR NMR to select glycyl peptide bonds. Only ^{13}C$-^{15}$N spin pairs in peptide bonds contribute to the 171 ppm ^{13}C{^{15}N} ΔS after dipolar evolution for 1.60 ms (Figure 2, top). These ^{13}C$-^{15}$N spin pairs include the glycyl carbonyl ^{13}C of [1-^{13}C,^{15}N]glycine that forms a peptide bond with the ^{15}N of another [1-^{13}C,^{15}N]glycine, or an isopeptide bond with L-[ε-^{15}N]lysine (Scheme 2). Hence, the 171 ppm peak amplitude (peak height) in the ΔS spectrum is directly proportional to the glycine content of

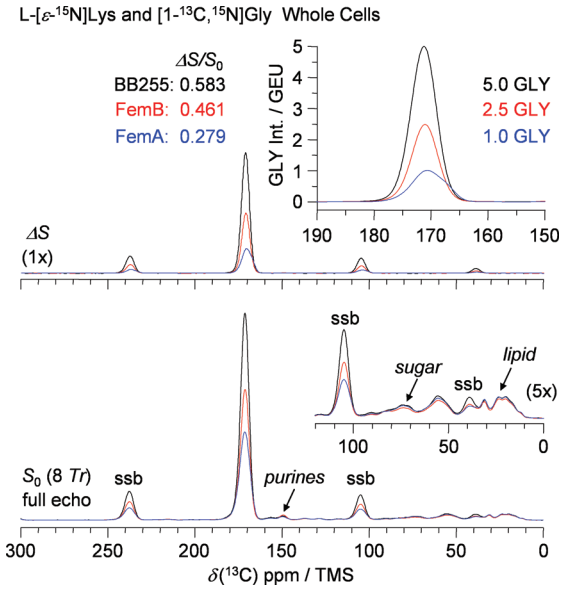

FIGURE 2: $^{13}C\{^{15}N\}$ REDOR spectra after $8T_r$ dipolar evolution (1.60 ms) obtained at 75 MHz with 5 kHz MAS of whole cells of wild-type *S. aureus* (BB255, black) and FemB (UT 34-2, red) and FemA (UK 17, blue) mutants labeled with [1-^{13}C,^{15}N]glycine and L-[ε-^{15}N]lysine. The full-echo spectra (S_0) are shown at the bottom of the figure, and the REDOR differences ($\Delta S = S_0 - S$, where S is the dephased echo) are shown at the top. Natural-abundance carbon peaks appear between 20 and 70 ppm in the S_0 spectrum (bottom inset). The 171 ppm peak height in the ΔS spectrum (top inset) of wild-type *S. aureus* BB255 was normalized to a five glycine-equivalent unit (GEU). The ^{13}C shoulder for FemA (top inset) is assigned to glycyl amines of open bridging segments with terminal NH_2 groups. The spectra were scaled according to the sample weight and total number of scans; ^{13}C chemical shifts are with respect to external tetramethylsilane (TMS).

the PG bridge structure. It is worth mentioning that the isotopic enrichment of glycine is stable over the different strains and do not affect the glycine content analysis (see descending paragraph). For wild-type *S. aureus*, there are five $^{13}C-^{15}N$ peptide bonds in the PG bridge structure that contribute to ΔS. Four $^{13}C-^{15}N$ peptide bonds are from four glycines in the glycine-glycine sequence, and the fifth is from the glycine-lysine bond (isopeptide bond) of the bridge link (Scheme 2). Because PG bridges shorter than five glycines constitute only a minor fraction in wild-type strains (*32*), the 171 ppm peak height in the ΔS spectrum of *S. aureus* BB255 was normalized to 5.0 (Figure 2, top inset). Thus, the corresponding glycine content in the PG of the FemB and FemA mutants is 2.5 ± 0.1 and 1.0 ± 0.1 glycine-equivalent units (GEU), respectively.

Although glycine-glycine peptide bonds in proteins also contribute to ΔS, this contribution is relatively small compared to that arising from the PG. First, the cytoplasmic dry weight is only two-thirds of the cell-wall dry weight (*33*). Second, the low frequency of glycine-glycine occurrences, estimated at 0.5% in protein (*34*), is minimal compared to the high frequency of glycine-glycine occurrences in PG of more then 50%. The relative protein contribution to ΔS increases in *fem*-deletion mutants due to the reduced number of glycines in the PG, but in all strains, the glycine-glycine contribution from protein to ΔS remains below the uncertainty associated with the ΔS measurement, which is less than 1%. The relative glycine incorporation into protein is estimated by subtracting ΔS (glycine exclusively in PG) from S_0 (total glycine content) and is approximately 42% for BB255, 54% for FemB, and 72% for FemA.

Bridge-Links in Cell-Wall Isolates. The 50 MHz $^{15}N\{^{13}C\}$ REDOR spectra of cell-wall isolates of wild-type *S. aureus* and its *fem*-deletion mutants labeled with [1-^{13}C]glycine and L-[ε-^{15}N]lysine are shown in Figure 3 (left). The ε-^{15}N-lysyl amide resonance is at 92 ppm and identifies a bridge-link to a PG glycine, while the ε-^{15}N-lysyl amine peak at 9 ppm is from a stem with no bridge attached. We assume that the level of incorporation of labeled lysine into undigested cell-wall protein is small compared to the level of incorporation in PG (*29*). Thus, the ratio of the 92 ppm to 9 ppm peak integrals in the S_0 spectrum is related to the degree of bridge-linking, ρ_{BL}, by

$$\frac{I(S_0^{\text{amide}})}{\alpha I(S_0^{\text{amine}})} = \frac{\rho_{BL}}{1 - \rho_{BL}}, \text{ where } \alpha = 1.2 \qquad (1)$$

The correction factor α was used to account for the differences in rotating-frame cross-polarization dynamics between amides and amines in lyophilized whole cells and cell walls (*35, 36*). These differences did not vary for BB255, FemB, and FemA. The integral of each peak was obtained as a function of cross-polarization contact time (*35, 36*). The values of ρ_{BL} for all strains are listed in Table 1. The errors are those of measuring the integrals which we estimate at ±2%.

Scheme 2: Distribution of Labels in the Cell-Wall Peptidoglycan of Wild-Type *S. aureus* and Its FemB and FemA Mutants, Grown in Defined Medium Containing [1-^{13}C,^{15}N]Glycine and L-[ε-^{15}N]Lysine

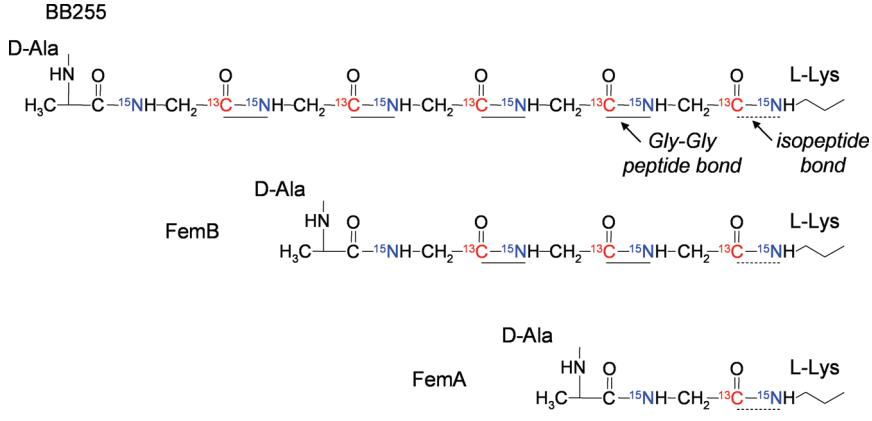

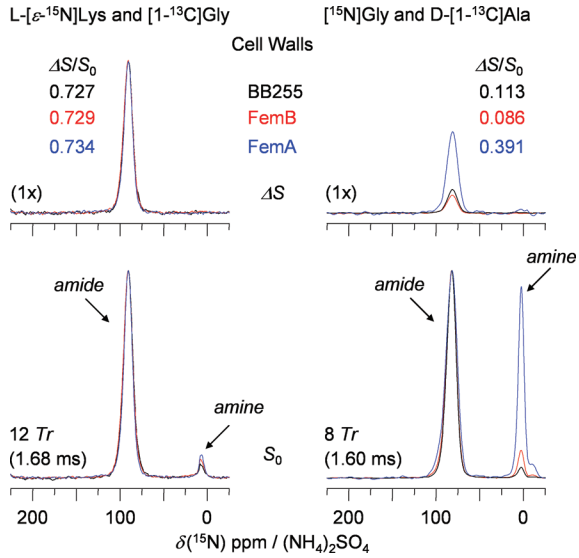

FIGURE 3: $^{15}N\{^{13}C\}$ REDOR spectra of cell-wall isolates of wild-type *S. aureus* (BB255, black) and its FemB (UT 34-2, red) and FemA (UK 17, blue) mutants labeled with (left) L-[ε-^{15}N]lysine and [1-^{13}C]glycine and (right) [^{15}N]glycine and D-[1-^{13}C]alanine. The full-echo spectra (S_0) are shown at the bottom of the figure, and the REDOR differences ($\Delta S = S_0 - S$, where S is the dephased echo) are shown at the top. The spectra on the left were obtained at 50 MHz with 7143 Hz MAS. After an evolution time of 1.68 ms, the amide peak at ~92 ppm is due to a lysyl bridge-link, and the amine peak at ~9 ppm is from an [ε-^{15}N]lysyl residue that is not bridge-linked. The spectra on the right were obtained at 30 MHz with 5 kHz MAS. After an evolution time of 1.60 ms, the amide peak at ~90 ppm is due to a glycyl-D-alanyl cross-link, and the amine peak at ~8 ppm is from a terminal glycyl bridging segment that is not cross-linked. ^{15}N chemical shifts are with respect to external ammonium sulfate [$(NH_4)_2SO_4$].

Cross-Links in Cell-Wall Isolates. The 30 MHz $^{15}N\{^{13}C\}$ REDOR spectra of cell-wall isolates of wild-type *S. aureus* and its *fem*-deletion mutants labeled with [^{15}N]glycine and D-[1-^{13}C]alanine are shown in Figure 3 (right). Wild-type *S. aureus* and its *FemB* mutant have a similar amide (~92 ppm) to amine (~9 ppm) S_0 ratio. In contrast, the FemA mutant shows a significant increase in the amine peak intensity, with an integrated amide-to-amine ratio of approximately 2:1. Therefore, FemA has a much higher percentage of glycyl amine, consistent with an increase in the number of uncross-linked (open) monoglycyl bridges in its PG. Open bridges are the likely source of the shoulder observed in the ^{13}C ΔS spectrum of FemA (Figure 2, top inset, blue).

The percentage of cross-linking, ρ_{CL}, was determined by comparing the S_0 amide-to-amine ratio for [^{15}N]glycine in isolated cell walls for all strains (Figure 3, bottom right). This is more direct than using the $^{15}N\{^{13}C\}$ $\Delta S/S_0$ which requires an accounting of the number of glycines contributing to S_0, the isotopic enrichment of D-Ala, and any leakage of D-[1-^{13}C]alanine label via pyruvate to [1-^{13}C]glycine. [Such scrambling was minimal because the resulting ^{13}C labeling of aliphatics in the cell-wall ^{13}C spectra was not observed (Figure S3, left panel, Supporting Information).]

The values of ρ_{CL} listed in Table 1 were obtained from

$$\frac{I(S_0^{\text{amide}})}{\alpha I(S_0^{\text{amine}})} = \frac{\rho_{CL} + (N-1)}{1-\rho_{CL}} \qquad (2)$$

where N is the experimentally determined average number of glycines in the PG-bridging segments for different strains. The glycyl amide peak in the S_0 spectra represents the cross-linked bridge, $I(S_0^{\text{amide}})$, (all glycyl peptide bonds in the cell-wall and attached cell-wall proteins), and the glycyl amine peak represents the uncross-linked bridges $I(S_0^{\text{amine}})$ in the PG. The factor α (equal to 1.2) accounted for differences in rotating-frame cross-polarization dynamics between amides and amines (*35, 36*). The errors in the ρ_{CL} values are ±2% (see above).

Isotopic Enrichment of Glycine and D*-Alanine.* The metabolic scrambling of labeled lysine is minimal (*21, 29*); hence, the level of ε-^{15}N (98%) isotopic enrichment is high and did not vary between strains. Isopeptide bonds between ε-^{15}N of lysine and glycyl carbonyl ^{13}C are only present in PG. The maximum $^{15}N\{^{13}C\}$ ΔS (observed after dipolar evolution for ~1.6 ms) was used to estimate the ^{13}C isotopic enrichment of the carbonyl ^{13}C of glycine, $f(^{13}C)$, of approximately 73% for all strains (Table 1). The enrichments measured from cell-wall isolates (Figure 3, left) were comparable to those inferred from measurements conducted on whole cells (Figure S2 of the Supporting Information). Dilution of incorporated [1-^{13}C]glycine is due to the endogenous glycine biosynthesis which also affected the ^{15}N isotopic enrichment of [^{15}N]glycine and [1-^{13}C,^{15}N]glycine (Table 1).

In the $^{15}N\{^{13}C\}$ ΔS spectra of Figure 3 (top right), only the [^{15}N]glycyl amide of the terminal [^{15}N]glycine that is cross-linked to the D-[^{13}C]alanine (Scheme 1) contributes to the 92 ppm peak during 1.60 ms of dipolar evolution. The four-bond penultimate glycyl contribution is negligible. The ^{13}C isotopic enrichment of D-[1-^{13}C]alanine, $f(^{13}C)$, is proportional to the dephasing value (ΔS^{amide}) divided by the scaled intensity of S_0 at 92 ppm, $I(^*S_0^{\text{amide}})$, and normalized by N

$$f(^{13}C) = \frac{1}{N}\frac{I(\Delta S^{\text{amide}})}{I(^*S_0^{\text{amide}})} \qquad (3)$$

The observed S_0 intensity at 92 ppm (S_0^{amide}) contains contributions from the [^{15}N]glycyl amides of both open and cross-linked bridges. The contribution from the [^{15}N]glycyl amides of open bridges is proportional to the number of [^{15}N]glycyl amides in the open bridges ($N - 1$), times the intensity of S_0 at 9 ppm (S_0^{amine}) so that

$$I(^*S_0^{\text{amide}}) = I(S_0^{\text{amide}}) - (N-1)I(S_0^{\text{amine}}) \qquad (4)$$

The estimated ^{13}C isotopic enrichments, $f(^{13}C)$, of incorporated D-[1-^{13}C]alanine for all strains using eqs 3 and 4 are listed in Table 1. The results of the D-alanine quantification in cell-wall isolates (Figures S3 and S4) and a description of this analysis are presented in the Supporting Information.

Whole Cells of S. aureus Fem Mutants. The interesting FemX mutant, which was investigated to have a complete overview of the *fem*-deletion mutants, is not part of our aim to understand the effect of bridge length on the 3-dimensional PG lattice in *S. aureus*. Results of experiments performed with FemX (Figures S5−S7) and a brief analysis are presented in the Supporting Information.

DISCUSSION

Transmission Electron Micrographs. The typical cell-wall thickness of wild-type *S. aureus* (BB255) measured by TEM

Table 1: Composition of Methicillin-Resistant Wild-Type *S. aureus* (BB255) and Its FemB (UT 34-2) and FemA (UK 17) Mutants

system	N^a (GEU)	$f(^{13}C)^b$ (Gly)	$f(^{15}N)^c$ (Gly)	$f(^{13}C)^d$ (D-Ala)	$\rho_{BL}{}^e$	$\rho_{CL}{}^f$	ρ^g
BB255	5.0[h]	0.73	0.73	0.73	0.94	0.80	0.75
FemB	2.5 ± 0.1	0.73	0.73	0.26	0.92	0.75	0.70
FemA	1.0 ± 0.1	0.73	0.73	0.37	0.91	0.62	0.57

[a] N is the average number of glycyl residues in a PG bridge structure, estimated from the ΔS amplitudes in Figure 2. [b] ^{13}C enrichment of incorporated [1-^{13}C]glycine. [c] ^{15}N enrichment of incorporated [^{15}N]glycine. [d] ^{13}C enrichment of incorporated D-[1-^{13}C]alanine determined by using eqs 3 and 4. [e] ρ_{BL} bridge-link degree determined by using eq 1. [f] ρ_{CL} cross-link degree determined by using eq 2. [g] Average degree of cross-linking is $\rho = \rho_{BL}\rho_{CL}$. The estimated error is ±4% based on the ±2% errors for ρ_{BL} and ρ_{CL}. [h] Wild-type *S. aureus* BB255 was normalized to a 5 glycine-equivalent unit (GEU).

is ~20 nm (*37*). The wild-type strain exhibited normal cell division without irregularities. However, in FemA (UK 17) and FemB (UT 34-2) mutants, irregular cell divisions were observed with "pseudomulticellular" (*37*) morphology. Multiple division planes in FemA are shown in Figure 1 (right, bottom). A premature septation associated with the formation of multiple, disorganized, and incomplete cross walls and an accumulation of PG material at the septum were also observed for both *fem*-deletion mutants. The partial thickening of the cross wall and the outer cell wall was the result of presumably immature (uncross-linked) PG accumulating at the septum. The splitting system is absent in *fem*-deletion mutants during cell division, which is in agreement with the literature (*37*). The loss of the ability to divide in *fem*-deletion mutants (*37*) is reflected in an unusually long lag-phase growth in both defined and complex media (Figure S1 of the Supporting Information).

Glycine Content of Cell Walls. The spectral profiles of ^{13}C natural-abundance peaks in the REDOR S_0 spectra (Figure 2, bottom) are similar, indicating that *fem* inactivation did not significantly alter cytoplasmic composition. Reduction in the carbonyl ^{13}C peak intensity at 171 ppm in *fem*-deletion mutants confirmed qualitatively that the level of incorporation of labeled glycine in whole cells was reduced. This reduction is primarily due to less glycine incorporation in the PG bridge structure by the mutants, as measured directly by $^{13}C\{^{15}N\}$ ΔS intensities (Figure 2, top). The GEUs for whole cells of FemB and FemA are 2.5 ± 0.1 and 1.0 ± 0.1, respectively. These measurements are comparable to the values reported by LC−MS analysis of cell-wall isolates, which are 2.6−2.9 for the FemB mutant (*13*) and 1.2 for the FemA mutant (*10*). However, the NMR measurements are not dependent on external calibration factors and are therefore inherently more accurate. The in situ measurement of 2.5 ± 0.1 GEU for the FemB mutant indicates a heterogeneous PG structure with 25% monoglycyl and 75% triglycyl bridges. This result is independent of a sampling bias and is a global average for whole cells.

Bridge-Links and Cross-Links. The reduction of PG-bridge lengths from 5.0 GEU (BB255) to 2.5 ± 0.1 GEU (FemB) to 1.0 ± 0.1 GEU (FemA) is associated with a decrease in the degree of cross-linking (ρ_{CL}) from 80 to 75 to 62%, respectively. The degree of bridge-linking (ρ_{BL}) remained stable, from 94 to 92 to 91%, respectively, consistent with the notion that the FemA and FemB proteins are not involved in the attachment of the first glycine in the PG bridge. The average degree of cross-link density (ρ), the product of ρ_{BL} and ρ_{CL}, therefore remained relatively stable for the wild-type strain and FemB, decreasing from 75 to 70%, but dropped to 57% for FemA. We believe that these cross-link densities are more accurate than estimates based on the LC−MS analysis of cell-wall digests, which are complicated by LC peaks representing multiple muropeptides of varying ionization efficiencies. This is a particularly acute problem in the LC−MS analysis of *S. aureus* because the high degree of cross-linking results in a wide range of mass fragments in the cell-wall digests.

The shortening of the bridge in FemB is associated with only modest changes in ρ_{CL} and ρ, although these changes could still be important. We speculate that a conformational change from a compact helical conformation observed for the pentaglycycl bridge structure in *S. aureus* (*21*) to a more extended bridge conformation in FemB could compensate for the shortening of the bridge. The only major difference in the results of Table 1 between the wild-type strain and FemB is the reduction of the level of isotopic enrichment of incorporated D-[1-^{13}C]alanine, from 75% in the wild-type strain to 26% in FemB. The cause of this reduction is unclear; however, the TEM images (Figure 1) show an accumulation of PG material at the septum implying an increased level of PG biosynthesis. This places a high demand on D-alanine, possibly accompanied by an increase in the level of endogenous alanine biosynthesis and a dilution of exogenous D-[1-^{13}C]alanine. A similar dilution was also observed for Fem*A* where the D-[1-^{13}C]alanine isotopic enrichment was reduced to 37%.

Combination of NMR and LC−MS. To investigate the PG tertiary structure of *S. aureus*, we propose a strategy of combining NMR analysis of intact cell walls with LC−MS analysis of digested cell walls. This strategy was first employed successfully in the characterization of the PG of *Enterococcus faecium* (*29*). Conditions for the gentle enzymatic digestion of the glycan sugars were found such that subsequent accurate mass measurements of unfragmented products led to a determination of total cross-linking in agreement with the solid-state NMR results. Because the usual prolonged period to ensure complete digestion could be avoided, structural modifications of the glycan sugars of the unfragmented products were still in place. These modifications are essential to an understanding of the complete cell-wall architecture of *S. aureus* and its *fem*-deletion mutants. We intend to use the compositions of Table 1 to help establish the least perturbative conditions for cell-wall digestions of wild-type methicillin-resistant *S. aureus* and its *fem*-deletion mutants.

Cell-Wall Composition and Architecture. A significant difference in cross-linking is observed between FemB and FemA mutants, a reduction from 70 to 57% (Table 1). Nevertheless, for FemA to achieve an average cross-link density as high as 57% with a short monoglycyl bridge, a rearrangement of cell-wall architecture seems likely. We believe that the transition from the tertiary PG structure in FemB to that in FemA represents a fundamental difference in the cell-wall structure of Gram-positive bacteria with long

bridges like (wild-type) *S. aureus*, and those with short bridges like *E. faecium* (*29*). This difference in tertiary PG structure certainly affects cell-wall biosynthesis and metabolism and may also affect cell morphology, drug permeability, and sensitivity to antimicrobial agents that target PG biosynthesis.

ACKNOWLEDGMENT

We thank Prof. Brigitte Berger-Bächi (Institut für Medizinische Mikrobiologie, Universität Zürich, Zurich, Switzerland) for providing wild-type and *fem*-deletion mutants of *S. aureus*, BB255, UK 17, UT 34-2, and SR-18, and W. Beatty of the Microbiology Imaging Facility at Washington University School of Medicine (St. Louis, MO) for the transmission electron micrographs.

SUPPORTING INFORMATION AVAILABLE

(i) Growth curves of the bacteria used in this report in defined medium (SASM); (ii) $^{15}N\{^{13}C\}$ REDOR spectra of whole cells of wild-type *S. aureus* (BB255), FemA, and FemB, enriched with L-[ε-^{15}N]lysine and [1-^{13}C]glycine or [^{15}N]glycine and D-[1-^{13}C]alanine; (iii) $^{13}C\{^{15}N\}$ REDOR spectra of cell-wall isolates enriched with [^{15}N]glycine and D-[1-^{13}C]alanine; (iv) complete accounting of cell-wall D-alanine, experimental deconvolution of the normalized 75 MHz carbonyl ^{13}C spectra of wild-type *S. aureus* (BB255) and FemB (UT 34-2) and FemA (UK 17) mutants labeled with [^{15}N]glycine and D-[1-^{13}C]alanine; (v) $^{15}N\{^{13}C\}$ REDOR spectra of whole cells of wild-type *S. aureus* (BB255) and its FemX mutant (SR 18) grown in media containing 1% D-(+)-glucose or D-(+)-xylose, and labeled with L-[ε-^{15}N]lysine and [1-^{13}C]glycine; (vi) $^{13}C\{^{15}N\}$ REDOR spectra of whole cells of wild-type *S. aureus* (BB255) and its FemX mutant (SR 18) labeled with L-[ε-^{15}N]lysine and [1-^{13}C]-glycine; (vii) $^{15}N\{^{13}C\}$ REDOR spectra of whole cells of wild-type *S. aureus* (BB255) grown in media containing 1% D-(+)-glucose or D-(+)-xylose and labeled with L-[ε-^{15}N]-lysine and [1-^{13}C]glycine; (viii) description of the D-alanine quantization in cell-wall isolates labeled with [^{15}N]glycine and D-[1-^{13}C]alanine; (ix) description of the FemX growth experiments; (x) sensitivity of the bacteria used in this report to lysostaphin and methicillin; and (xi) tabulated selected REDOR dephasing values for both the main text and supporting material. This material is available free of charge via the Internet at http://pubs.acs.org.

REFERENCES

1. Hiramatsu, K., Cui, L., Kuroda, M., and Ito, T. (2001) The emergence and evolution of methicillin-resistant *Staphylococcus aureus*. *Trends Microbiol. 9*, 486–493.
2. Labischinski, H. (1992) Consequences of the interaction of β-lactam antibiotics with penicillin-binding proteins from sensitive and resistant *Staphylococcus aureus* strains. *Med. Microbiol. Immunol. 181*, 241–265.
3. Ubukata, K., Nonoguchi, R., Matsuhashi, M., and Konno, M. (1989) Expression and inducibility in *Staphylococcus aureus* of the *mecA* gene, which encodes a methicillin-resistant *S. aureus*-specific penicillin-binding protein. *J. Bacteriol. 171*, 2882–2885.
4. Rohrer, S., and Berger-Bächi, B. (2003) *FemABX* peptidyl transferases: A link between branched-chain cell wall peptide formation and β-lactam resistance in Gram-positive *cocci*. *Antimicrob. Agents Chemother. 47*, 837–846.
5. Berger-Bächi, B., and Tschierske, M. (1998) Role of *Fem* factors in methicillin resistance. *Drug Resist. Updates 1*, 325–335.
6. Labischinski, H., Ehlert, K., and Berger-Bächi, B. (1998) The targeting of factors necessary for expression of methicillin resistance in *staphylococci*. *J. Antimicrob. Chemother. 41*, 581–584.
7. de Lencastre, H., Jonge, B. L. M., Matthews, P. R., and Tomasz, A. (1994) Review molecular aspects of methicillin resistance in *Staphylococcus aureus*. *J. Antimicrob. Chemother. 33*, 7–14.
8. Rohrer, S., Ehlert, K., Tschierske, M., Labischinski, H., and Berger-Bächi, B. (1999) The essential *Staphylococcus aureus* gene *fmhB* is involved in the first step of peptidoglycan pentaglycine interpeptide formation. *Proc. Natl. Acad. Sci. U.S.A. 96*, 9351–9356.
9. Tschierske, M., Mori, C., Rohrer, S., Ehlert, K., Shaw, K. J., and Berger-Bächi, B. (1999) Identification of three additional *femAB*-like open reading frames in *Staphylococcus aureus*. *FEMS Microbiol. Lett. 171*, 97–102.
10. Ehlert, K., Schröder, W., and Labischinski, H. (1997) Specificities of *FemA* and *FemB* for different glycine residues: *FemB* cannot substitute for *FemA* in *staphylococcal* peptidoglycan pentaglycine side chain formation. *J. Bacteriol. 179*, 7573–7576.
11. Kopp, U., Roos, M., Wecke, J., and Labischinski, H. (1996) *Staphylococcal* peptidoglycan interpeptide bridge biosynthesis: A novel antistaphylococcal target. *Microb. Drug Resist. 2*, 29–41.
12. Maidhof, H., Reinicke, B., Blümel, P., Berger-Baechi, B., and Labischinski, H. (1991) *femA*, which encodes a factor essential for expression of methicillin resistance, affects glycine content of peptidoglycan in methicillin-resistant and methicillin-susceptible *Staphylococcus aureus* strains. *J. Bacteriol. 173*, 3507–3513.
13. Henze, U., Sidow, T., Wecke, J., Labischinski, H., and Berger-Baechi, B. (1993) Influence of *femB* on methicillin resistance and peptidoglycan metabolism in *Staphylococcus aureus*. *J. Bacteriol. 175*, 1612–1620.
14. Hübscher, J., Jansen, A., Kotte, O., Schäfer, J., Majcherczyk Paul, A., Harris Llinos, G., Bierbaum, G., Heinemann, M., and Berger-Bächi, B. (2007) Living with an imperfect cell wall: Compensation of *femAB* inactivation in *Staphylococcus aureus*. *BMC Genomics 8*, 307.
15. Ling, B., and Berger-Bächi, B. (1998) Increased overall antibiotic susceptibility in *Staphylococcus aureus femAB* null mutants. *Antimicrob. Agents Chemother. 42*, 936–938.
16. Strandén, A. M., Ehlert, K., Labischinski, H., and Berger-Bächi, B. (1997) Cell wall monoglycine cross-bridges and methicillin hypersusceptibility in a *femAB* null mutant of methicillin-resistant *Staphylococcus aureus*. *J. Bacteriol. 179*, 9–16.
17. Rogers, H. J., Perkins, H. R., and Ward, J. B. (1980) *Microbial Cell Walls and Membranes*, Chapman and Hall, London.
18. Berger-Bächi, B. (1983) Insertional inactivation of *staphylococcal* methicillin resistance by Tn551. *J. Bacteriol. 154*, 479–487.
19. Cegelski, L., Stueber, D., Mehta, A. K., Kulp, D. W., Axelsen, P. H., and Schaefer, J. (2006) Conformational and Quantitative Characterization of Oritavancin-Peptidoglycan Complexes in Whole Cells of *Staphylococcus aureus* by in Vivo ^{13}C and ^{15}N Labeling. *J. Mol. Biol. 357*, 1253–1262.
20. Kim, S. J., Cegelski, L., Studelska, D. R., O'Connor, R. D., Mehta, A. K., and Schaefer, J. (2002) Rotational-echo double resonance characterization of vancomycin binding sites in *Staphylococcus aureus*. *Biochemistry 41*, 6967–6977.
21. Tong, G., Pan, Y., Dong, H., Pryor, R., Wilson, G. E., and Schaefer, J. (1997) Structure and dynamics of pentaglycyl bridges in the cell walls of *Staphylococcus aureus* by ^{13}C-^{15}N REDOR NMR. *Biochemistry 36*, 9859–9866.
22. Schaefer, J., and McKay, R. A. (1999) Multi-Tuned Single-Coil Transmission-Line Probe for Nuclear Magnetic Resonance Spectrometer. U.S. Patent 5,861,748.
23. Stueber, D., Mehta, A. K., Chen, Z., Wooley, K. L., and Schaefer, J. (2006) Local order in polycarbonate glasses by $^{13}C\{^{19}F\}$ rotational-echo double-resonance NMR. *J. Polym. Sci. Phys. 44*, 2760–2775.
24. Bennett, A. E., Rienstra, C. M., Auger, M., Lakshmi, K. V., and Griffin, R. G. (1995) Heteronuclear decoupling in rotating solids. *J. Chem. Phys. 103*, 6951–6958.
25. Gullion, T., and Schaefer, J. (1989) Detection of weak heteronuclear dipolar coupling by rotational-echo double-resonance nuclear magnetic resonance. *Adv. Magn. Reson. 13*, 57–83.
26. Gullion, T., and Schaefer, J. (1989) Rotational-echo double-resonance NMR. *J. Magn. Reson. 81*, 196–200.
27. Lewandowski, J. R., De Paëpe, G., and Griffin, R. G. (2007) Proton Assisted Insensitive Nuclei Cross Polarization. *J. Am. Chem. Soc. 129*, 728–729.
28. Kim, S. J., Matsuoka, S., Patti, G. J., and Schaefer, J. (2008) Vancomycin derivative with damaged D-Ala-D-Ala binding cleft

binds to cross-linked peptidoglycan in the cell wall of *Staphylococcus aureus*. *Biochemistry 47*, 3822–3831.
29. Patti, G. J., Kim, S. J., and Schaefer, J. (2008) Characterization of the peptidoglycan of vancomycin-susceptible *Enterococcus faecium*. *Biochemistry 47*, 8378–8385.
30. Pasciak, M., Holst, O., Lindner, B., Mordarska, H., and Gamian, A. (2003) Novel bacterial polar lipids containing ether-linked alkyl chains, the structures and biological properties of the four major glycolipids from *Propionibacterium propionicum* PCM 2431 (ATCC 14157T). *J. Biol. Chem. 278*, 3948–3956.
31. Kim, S. J., Cegelski, L., Preobrazhenskaya, M., and Schaefer, J. (2006) Structures of *Staphylococcus aureus* Cell-Wall Complexes with Vancomycin, Eremomycin, and Chloroeremomycin Derivatives by $^{13}C\{^{19}F\}$ and $^{15}N\{^{19}F\}$ Rotational-Echo Double Resonance. *Biochemistry 45*, 5235–5250.
32. Roos, M., Pittenauer, E., Schmid, E., Beyer, M., Reinike, B., Allmaier, G., and Labischinski, H. (1998) Improved high-performance liquid chromatographic separation of peptidoglycan isolated from various *Staphylococcus aureus* strains for mass spectrometric characterization. *J. Chromatogr., B 705*, 183–192.
33. Wyatt, P. J. (1970) Cell wall thickness, size distribution, refractive index ratio and dry weight content of living bacteria (*Staphylococcus aureus*). *Nature 226*, 277–279.
34. McCaldon, P., and Argos, P. (1988) Oligopeptide biases in protein sequences and their use in predicting protein coding regions in nucleotide sequences. *Proteins: Struct., Funct., Genet. 4*, 99–122.
35. McDowell, L. M., Schmidt, A., Cohen, E. R., Studelska, D. R., and Schaefer, J. (1996) Structural constraints on the ternary complex of 5-enolpyruvylshikimate-3-phosphate synthase from rotational-echo double-resonance NMR. *J. Mol. Biol. 256*, 160–171.
36. Pan, Y., Shenouda, N. S., Wilson, G. E., and Schaefer, J. (1993) Cross-links in cell walls of *Bacillus subtilis* by rotational-echo double-resonance ^{15}N NMR. *J. Biol. Chem. 268*, 18692–18695.
37. Giesbrecht, P., Kersten, T., Maidhof, H., and Wecke, J. (1998) *Staphylococcal* cell wall: Morphogenesis and fatal variations in the presence of penicillin. *Microbiol. Mol. Biol. Rev. 62*, 1371–1414.

BI801750U